

Figure S1. A comparison between the X-ray structure of the COVID-19-ACE2 complex (PDB 6VW1, pink) and the molecular dynamics (MD) trajectory frames. The MD snapshots are colored gray and blue for ACE2 and COVID-19 RBD, respectively. The average RMSD over the interface C α atoms is ~1Å.

HCoV-NL63	481	QHTDINF	TATAS	FGGSCY	VCKPHQ	VNISL	NG-----	NTSVC-----	VRT
MERS	381	VECDF	SPLLS	SGTP-	PQVYN	FKRLV	TNCN	YNLT	KLKLSLFSVNDFTC-----
COVID-19	334	--CPFGE	VFNAT	RFASV	YAWNR	KRISN	CVADY	SVLYNS	ASFSTFKCYGVSPTKLNDLCFT
SARS-2002	321	--CPFGE	VFNAT	KFPSV	YAWER	KKISN	CVADY	SVLYNST	FFSTFKCYGVSATKLNDLCFS
SARS-des	321	--CPFGE	VFNAT	KFPSV	YAWER	KKISN	CVADY	SVLYNST	FFSTFKCYGVSATKLNDLCFS
		:	.	:	.	*	:	.	.
		:	.	:	.	*	:	.	.
HCoV-NL63	520	SHFSIRY	IY----	NRVKS	SGSPG--	DSSWH	IYLK	SGTC-----	PFSFSK
MERS	440	SLILDY	FSYPL	SMKSD	LSVSS	AGPIS	QFNY	KQSF	SNPTCLILATVPHNLTITIKPLKYSY
COVID-19	388	NVYADS	SVIRG	DEVQR	IAPGQ	TGKI	ADYNY	KLPDD	FTGCVIAWNSNNLDSKVGGN
SARS-2002	375	NVYADS	SVVVK	GDDVR	QIAPG	QTGV	IADYNY	KLPDD	FMGCVLAWNTNIDATSTGN
SARS-des	375	NVYADS	SVVVK	GDDVR	QIAPG	QTGV	IADYNY	KLPDD	FMGCVLAWNTNIDATSTGN
		.	:	:
		.	:	:
HCoV-NL63	553	----	LNNFQ	KF----	KTICF	STVE--	-----	VPGSCN	FPLEATWHYTSYTIVGALYV
MERS	500	----	INKSR	FLSDD	TEVPQ	LVNAN	QYSP	CVSIV	PSTV-WEDGDYYKQLSPLEGGGWL
COVID-19	454	RLFRK	SNLKP	PFERD	ISTEY	QAGS---	TPCNG	VEGF	NCYFPLOS--YGFQPTNGVGYQ
SARS-2002	441	RYLRH	GKLRP	PFERD	ISNV	PFSPD	G----	KPCTP-	PALNCYWPLND--YGFYTTTGIGYQ
SARS-des	441	RFLRH	GKLRP	PFERD	ISNV	PFSPD	G----	KPCTP-	PAFNCYWPLND--YGFYTTTGIGYQ
		.	:	*
		.	:	*
HCoV-NL63	599	TWSE	-----	-----	-----	-----	-----	-----	-----
MERS	555	VASGST	VAMTE	QLQM	GFGIT	VQYG	-----	-----	-----
COVID-19	507	PYRV	-----	-----	-----	-----	-----	-----	-----
SARS-2002	493	PYRV	-----	-----	-----	-----	-----	-----	-----
SARS-des	493	PYRV	-----	-----	-----	-----	-----	-----	-----

Figure S2. The multiple sequence alignment of the analyzed receptor-binding domains (RBDs).

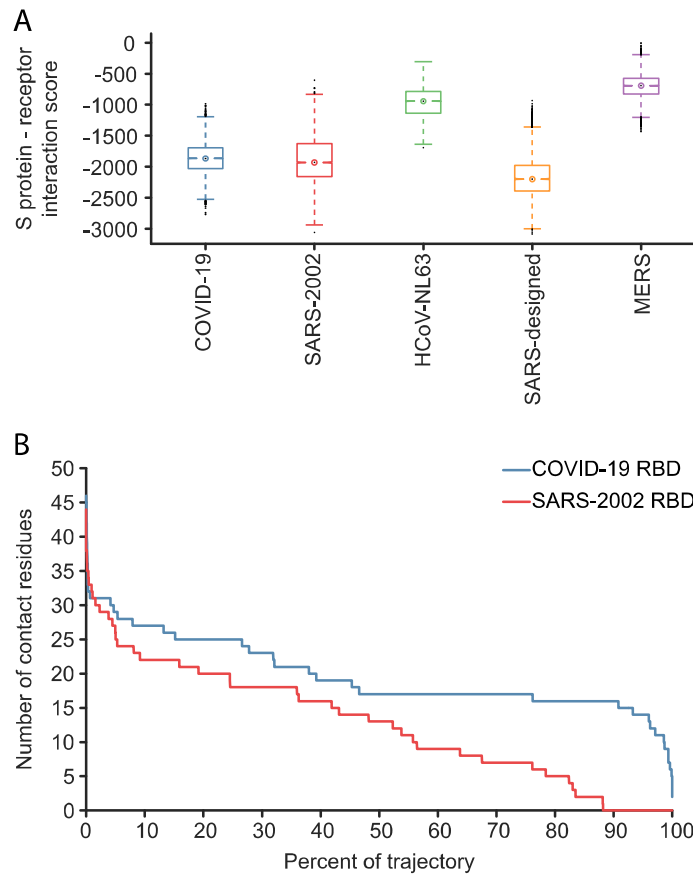


Figure S3. (A) Box plots of the statistically optimized atomic potentials (SOAP) interaction scores for the trajectory's frames. The center point is the median score, while 50% of the scores are within the box. The whiskers extend to cover > 99% of the scores. (B) The numbers of RBD residues in contact with ACE2 vs. the fraction of trajectory frames for COVID-19 (blue) and SARS-2002 (red).

COVID-19	Residue number	SARS-2002	Residue number
ARG	403	LYS	390
LYS	417	VAL	404
VAL	445	SER	432
GLY	446	THR	433
LEU	455	TYR	442
PHE	456	LEU	443
TYR	473	PHE	460
GLN	474	SER	461
ALA	475	PRO	462
GLY	476	ASP	463
SER	477	GLY	464
THR	478	LYS	465
ASN	481	THR	468
GLY	482	PRO	469
GLU	484	PRO	470
GLY	485	ALA	471
PHE	486	LEU	472
PHE	490	TRP	476
GLN	493	ASN	479
SER	494	ASP	480
GLN	498	TYR	484
PRO	499	THR	485
ASN	501	THR	487
VAL	503	ILE	489

Table S1. The receptor-binding domain (RBD) interface residues that have substitutions between COVID-19 and SARS-2002.

	PRODIGY ΔG (kcal mol ⁻¹) ¹⁾	PRODIGY Kd 10 ⁻⁹ (M)	FoldX (kcal/mol ⁻¹)	SOAP score
COVID-19—ACE2	-11.7	2.60	-1.93	-1865.9
SARS-2002— ACE2	-12.1	1.30	-2.67	-1929.5

Table S2. RBD–ACE2 interface evaluated by several methods for analysis of protein–protein interactions.

Movie S1. The overlay of 50 random snapshots from the MD trajectories of COVID-19–ACE2, SARS-2002–ACE2, and HCoV-NL63–ACE2 complexes. For clarity, only one copy of the ACE2 is shown (gray), and COVID-19, SARS-2002, and HCoV-NL63 are colored blue, red, and green, respectively.